Радиофизика и радиоастрономия, 2000, т. 5, №3, стр. 301-310

Noise Reduction Algorithm Based on Template Wavelet Coefficients

O. O. Bezvesilniy, V. V. Vinogradov, and K. Sch˘nemann[1]

Institute of Radio Astronomy, NAS of Ukraine
4 Chervonopraporna St., 61002 Kharkiv, Ukraine

[1]Institute of Microwave Engineering, Technical University
Hamburg-Harburg, D-21071 Hamburg, Germany

Received November 3, 2000

In the paper, a new algorithm based on the application of template wavelet coefficients is proposed to solve the problems concerning noise reduction in the vicinity of edges in signals and images and suppressing parasitic oscillations, which arise when threshold wavelet algorithms are used. It is shown that this approach calls for choosing a specific wavelet. Examples of the application of the developed technique are given.

1. Introduction

The problem on noise reduction and enhancement of image edges ranks among typical problems in image processing. This paper deals with the problem of noise reduction in signals, which are slowly varying functions between sharp edges. The strings and columns of images obtained in experiments or observations are examples of such signals. For instance, radar images of clouds have slowly varying reflectivity between sharp cloud edges.

The high-frequency noise components produce the main distortions in signals and images, since the power of the signal high-frequency component is often less than the power of the low-frequency component. However, an application of the conventional low-frequency filtration results in smoothing edges and loosing fine features. To keep the edge sharpness, the high frequencies should be removed between the edges and retained in the vicinities of the edges. For this purpose, one can use a representation of the signal, which allows analyzing local properties of signals both in time and frequency domain. Window Fourier transform is an example of such representation [1],

$$\hat{f}(\omega,b)=\frac{1}{\sqrt{2\pi}}\int_{-\infty}^{\infty} f(t)\,w(t-b)\,\mathrm{e}^{-i\omega t}\,\mathrm{d}t.$$

Here $w(t)$ is a window function, usually Gaussian. Window Fourier transform gives the spectrum of the part of a signal cut out by the “window”. A disadvantage of this transform is that the time resolution determined by the window width is fixed. Wavelet transforms provide more accurate time-frequency representation of signals.

Wavelet is a square integrable function localized both in time and frequency domain and satisfing the admissibility condition [1]

$$C_\psi=\int_{-\infty}^{\infty}\frac{|\hat{\psi}(\omega)|^2}{\omega}\mathrm{d}\omega<\infty.$$

If wavelet is a differentiable function, the admissibility condition can be rewritten as

$$\int_{-\infty}^{\infty}\psi(t)\mathrm{d}t=0. \qquad (1)$$

Classical examples of wavelets are the first and the second derivatives of the Gaussian,

$$\psi(t)=t\exp\left(-t^2\right), \qquad \psi(t)=\left(1-2t^2\right)\exp\left(-t^2\right).$$

The continuous wavelet transform (CWT) of a signal $f(t)$ is introduced as [1-5]

$$W(a,b)=\int_{-\infty}^{\infty} f(t)\psi^*_{a,b}(t)\mathrm{d}t,\quad \psi_{a,b}(t)=\frac{1}{\sqrt{a}}\psi\left(\frac{t-b}{a}\right), \tag{2}$$

where b denotes the real numbers, and a is a positive number. The symbol "*" stands for complex conjugation. If the admissibility condition is satisfied, the inverse continuous wavelet transform is given by the relation

$$f(t)=\frac{1}{C_\psi}\int_{-\infty}^{\infty}\int_{-\infty}^{\infty} W(a,b)\psi_{a,b}(t)\frac{\mathrm{d}a\mathrm{d}b}{a^2}.$$

The wavelet spectrum $W(a,b)$ is a function of two variables: the scale parameter $a > 0$ (the analog of frequency) and translation parameter b (location of the time window). The wavelet transform gives a local spectrum of signal in the vicinity of b, similarly to the window Fourier transform. However, the time and frequency resolutions of the wavelet transform are related to each other: the high-frequency wavelet has a narrow time window and low-frequency wavelet has a wide time window. It should be also noted that there are a lot of different wavelets and one can choose an appropriate wavelet allowing for the features of the problem considered.

In practice, the discrete wavelet transform (DWT) is usually applied [1-6], in which case the samples of the wavelet spectrum, called wavelet coefficients, are calculated. Samples of the wavelet spectrum are taken in the nodes of a grid on the plane (a,b),

$$d_j[k]=W(a_j,b_{j,k}),\qquad j,k\in Z. \tag{3a}$$

where Z denotes the space of integer numbers.

There are two types of discrete wavelet transforms and wavelet coefficients: decimated and undecimated, depending on the type of the grid.The former DWT calculates the samples of the wavelet spectrum on the following grid:

$$a_j=2^j,\qquad b_{j,k}=2^j k,$$

whereas the latter – on the grid:

$$a_j=2^j,\qquad b_k=k, \tag{3b}$$

Wavelet coefficients with the same octave number j and various k-values form an octave.

The inverse discrete wavelet transform was introduced to reconstruct the original signal from its wavelet coefficients.

Several algorithms based on the wavelet transform have been proposed to treat signals and images (e. g. [7-9]). Each algorithm involves three main steps: i) The wavelet spectrum is formed using some type of wavelet transform. ii) Then the spectrum is treated by means of linear or nonlinear filtration. iii) Finally, an inverse wavelet transformation is performed to get the filtered image or signal.

From (1) and (2) one can conclude that the smaller signal variation, the smaller the values of the wavelet coefficients, and vice versa. This means that sharp variations of a signal or image edges give rise to peaks in each octave of the wavelet coefficients. Such peaks are called edge peaks. Their position indicates location of edges. The presence of noise leads to similar peaks and naturally complicates the analysis. Examples of wavelet coefficients for clean and noisy signals are given in Fig. 1.

The main idea of so far used algorithms for filtration of the wavelet coefficients lies in the following. The wavelet coefficients that describe the edge peaks are preserved, whereas the rest of the coefficients are eliminated. This leads to reduction of noise influence. The difference between various algorithms is mainly due to the rule, which is used to determine the correct coefficients describing the edge peaks.

The wavelet threshold filtering is the most popular algorithm for this purpose. According to this algorithm, the wavelet coefficients, which exceed some threshold value, are considered as correct ones. The threshold value is chosen either heuristically or with the help of special algorithms [7, 8].

This approach has two disadvantages. Firstly, deleting the "damping tail" of edge peaks leads to parasitic oscillations in the reconstructed signal. Secondly, the coefficients satisfying the threshold condition are not eliminated, so that the noise in the vicinity of edges is not filtered.

The drawbacks mentioned are illustrated in Figs. 2 and 3. The result of the application of threshold filtering to the noiseless test signal of Fig. 2 (a) is shown in Fig. 2 (b). The parasitic oscillations due to deleting the "damping tail" is clearly seen in the latter figure. Fig. 3 illustrates the application of this approach to a noisy test signal shown in Fig. 3 (a). The result of the filtration depicted in Fig. 3 (b) illustrates that the noise in the vicinity of edges is preserved.

In this paper, a novel approach to the filtration of wavelet coefficients is proposed in order to get rid of

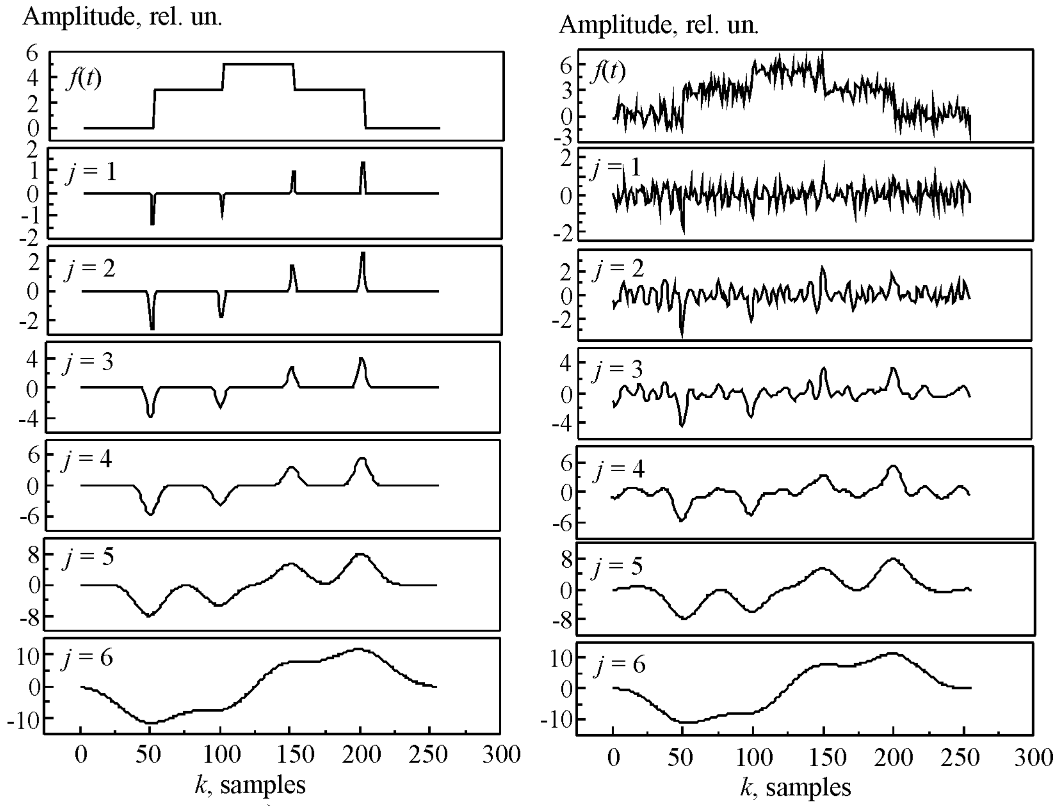

a) b)

Fig. 1. *The wavelet coefficients $d_j[k]$ of the signal f(t): clean (a) and noisy (b)*

these drawbacks. The main idea of the approach lies in the application of template wavelet coefficients, which are used for replacing the noisy wavelet coefficients. To realize the technique proposed a specific type of analyzing wavelet should be used. It has been found that the first derivative of the cubic B-spline is an appropriate choice for analyzing wavelet.

The paper is organized as follows. The elements of the theory of multiresolution analysis (MMA) are considered and the formulas of undecimated DWT are given in Section 2. The main idea of the proposed algorithm is described in Section 3. In Section 4, the choice of the analyzing wavelet is discussed. Section 5 contains a conclusion.

2. Multiresolution Analysis and Discrete Wavelet Transform

In this paper, we consider the DWT algorithms based on multiresolution analysis (MRA) and the pyramidal algorithms similar to them. The rigorous mathematical definition of MRA can be found in [1, 6]. Here we give a simplified definition of MRA, sufficient to explain the DWT algorithm.

In the theory of MRA a square integrable function *f*(*t*) is represented as a sequence of its approximations $f_j(t)$. The larger octave number *j*, the smoother the approximation $f_j(t)$. In other words, more accurate approximation (with smaller *j*) contains higher frequencies; the accuracy of the approximation increases with improving the resolution.

MRA is defined as a sequence of closed nested subspaces $V_j \subset L^2(R)$, where *R* is the space of the real numbers,

$$\ldots \subset V_2 \subset V_1 \subset V_0 \subset V_{-1} \subset \ldots,$$

and the approximations $f_j(t)$ are the projections of $f(t) \in L^2(R)$ on each of the subspaces V_j. Let us de-

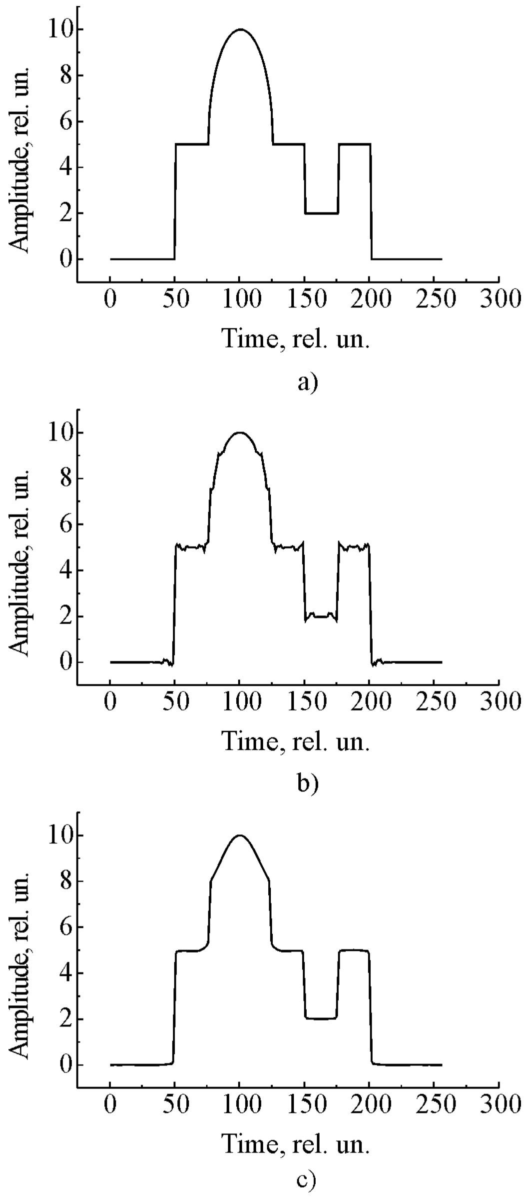

Fig. 2. *Noiseless test signal processing:*
(a) – noiseless test signal, (b) – test signal after threshold filtering, (c) – test signal after the proposed filtering technique

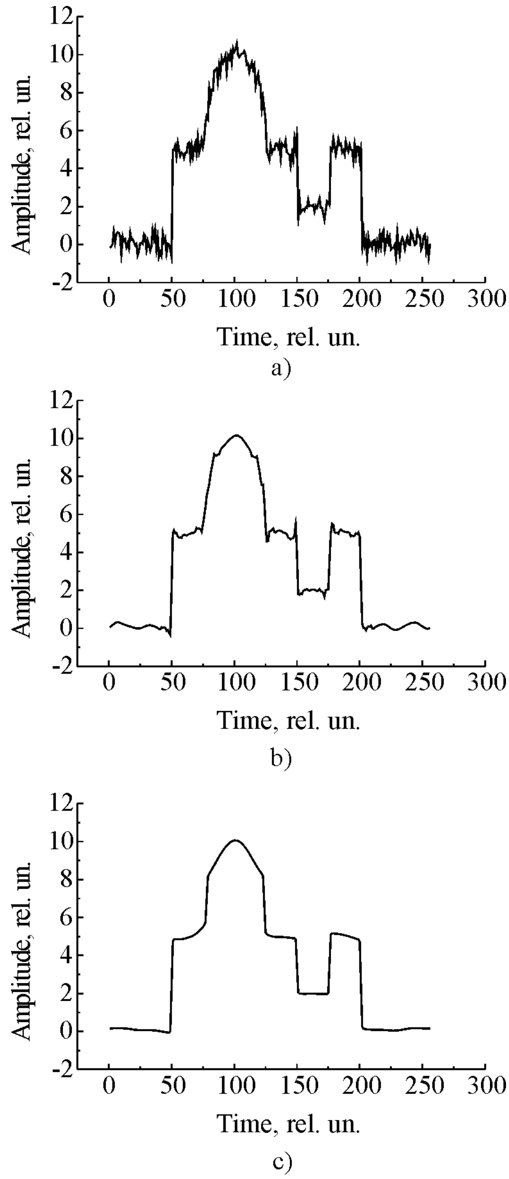

Fig. 3. *Noisy test signal filtering:*
(a) – noisy test signal, (b) – test signal after threshold filtering, (c) – test signal after the proposed filtering technique

note the orthogonal complement of V_j to V_{j-1} as W_j,

$$V_{j-1} = V_j \oplus W_j .$$

The symbol of the direct sum means that each element of the subspace V_{j-1} can be uniquely written as a sum of an element of V_j and an element of W_j. The subspace W_j contains the "detail" information required to go from the approximation with the resolution j to the approximation with the resolution $j-1$.

In each of the subspaces V_j there exists an orthogonal basis [1],

$$\left\{\phi_{j,k}(t)\right\}_{k\in Z}, \qquad \phi_{j,k}(t) = \frac{1}{\sqrt{2^j}}\phi\left(\frac{t-2^j k}{2^j}\right).$$

Square integrable function $\phi(t)$ is a scaling function of the MRA and satisfies the requirement

$$\int_{-\infty}^{\infty} \phi(t)\mathrm{d}t = 1 .$$

In subspaces W_j there exists an orthogonal wavelet basis,

$$\{\psi_{j,k}(t)\}_{k\in Z}, \qquad \psi_{j,k}(t) = \frac{1}{\sqrt{2^j}}\psi\left(\frac{t-2^j k}{2^j}\right).$$

It should be noted that such basis could not be formed by an arbitrary wavelet, but only by some special wavelets.

The MRA described above is an orthogonal one: $W_j \perp V_j$. There exists a biorthogonal MRA with the sequences of dual subspaces $\tilde{V}_j$ and $\tilde{W}_j$, and therefore $\tilde{W}_j \perp V_j$, $W_j \perp \tilde{V}_j$. Bases in the subspaces $\tilde{V}_j$ and $\tilde{W}_j$ are formed by dual scaling function $\tilde{\phi}$ and dual wavelet $\tilde{\psi}$, respectively.

The subspace $\tilde{V}_0$ can be represented as a direct sum of $\tilde{V}_1$ and $\tilde{W}_1$, then the subspace $\tilde{V}_1$ can be represented as a direct sum of $\tilde{V}_2$ and $\tilde{W}_2$, and so on, and we have

$$\tilde{V}_0 = \tilde{V}_J \oplus \bigoplus_{j=1}^{J} \tilde{W}_j$$

$$f_0(t) = \sum_k c_J[k]\tilde{\phi}_{J,k}(t) + \sum_{j=1}^{J}\sum_k d_j[k]\tilde{\psi}_{j,k}(t) .$$

The coefficients

$$c_J[k] = \int_{-\infty}^{\infty} f(t)\phi^*_{J,k}(t)\mathrm{d}t$$

are called the scaling coefficients of the function $f(t)$. Thus, signal is exactly described by its wavelet coefficients $d_j[k]$, $j = 1, 2, ..., J$ and scaling coefficients $c_J[k]$. Scaling coefficients give low-frequency smooth approximation, whereas wavelet coefficients describe fine features and edges.

In practice, signal can be measured and presented by its samples only approximately. The signal measured can be projected on the subspace V_0 and we will assume that the approximation $f_0(t)$ is sufficiently accurate. The scaling function $\phi(t)$ is well localized both in time and frequency domain similar to wavelet, and, therefore, the scaling coefficients $c_0[k]$ can be considered as the samples of the signal with sufficient accuracy.

According to the expression

$$V_{-1} = V_0 \oplus W_0 ,$$

the basis functions of the subspaces V_0 and W_0 can be expanded via the basis functions of the subspace V_{-1},

$$\phi(t) = \sqrt{2}\sum_k h[k]\phi(2t-k) , \qquad (4a)$$

$$\psi(t) = \sqrt{2}\sum_k g[k]\phi(2t-k) , \qquad (4b)$$

and the basis functions of the subspace V_{-1} – via the basis functions of the subspaces V_0 and W_0,

$$\sqrt{2}\phi(2t-n) = \sum_k \tilde{h}[n-2k]\phi(t-k) + $$
$$+ \sum_k \tilde{g}[n-2k]\psi(t-k) . \qquad (4c)$$

Here h, g, $\tilde{h}$, and $\tilde{g}$ are the filters determined by the wavelet and the scaling function.

Relations (4a-4b) enable to build fast recursive undecimated DWT algorithm [1, 4-6] called the DWT algorithm based on MRA. The pyramidal DWT algorithms are based on the other recursive relations similar to recursive relations of MRA (4).

An algorithm of the direct undecimated DWT is given by

$$c_{j+1}[k] = \sum_n h^*[n]c_j[k+2^j n] , \qquad (5a)$$

$$d_{j+1}[k] = \sum_n g^*[n]c_j[k+2^j n] , \qquad (5b)$$

and allows to calculate recursively the coefficients $d_j[k]$, $j = 1, 2, ..., J$, and $c_J[k]$ from the scaling coefficients $c_0[k]$,

$$c_0[k] = \int_{-\infty}^{\infty} f(t)\phi^*(t-k)\mathrm{d}t.$$

An inverse undecimated DWT algorithm is given by

$$c_j[k] = \frac{1}{2}\sum_n \tilde{h}[n]c_{j+1}[k-2^j n] + \frac{1}{2}\sum_n \tilde{g}[n]d_{j+1}[k-2^j n], \quad (5c)$$

and yields the coefficients $c_0[k]$ from the coefficients $d_j[k]$, $j = 1, 2, ..., J$, and $c_J[k]$.

3. The Algorithm of Template Wavelet Coeffcients

Since wavelet coefficients are the result of the convolution of the wavelet and signal, the shape of the edge peak is determined by the shape of both the wavelet and edge. The jump is the simplest edge and a signal with such single edge is the Heaviside function

$$\theta(t) = \begin{cases} 1, & t \geq 0, \\ 0, & t < 0. \end{cases}$$

In accordance with (2), (3), the undecimated wavelet coefficients of the Heaviside function, called below the template wavelet coefficients, are given by

$$d_j^{\theta}[k] = \frac{1}{\sqrt{2^j}}\int_{-k}^{\infty} \psi^*\left(\frac{t}{2^j}\right)\mathrm{d}t. \quad (6)$$

These coefficients describe the edge peaks, which correspond to a jump discontinuity of unit height for any function.

Let us consider a signal, which is a slowly changing function between sharp edges. Such signal can be represented as

$$f(t) = s(t) + \sum_m H_m\theta(t-T_m),$$

where $s(t)$ is a slowly varying function, T_m and H_m are the coordinates and heights of the sharp edges. The wavelet coefficients of such signal are given by

$$d_j[k] = \frac{1}{\sqrt{2^j}}\int_{-\infty}^{\infty} s(t)\psi^*\left(\frac{t-k}{2^j}\right)\mathrm{d}t + \\ + \frac{1}{\sqrt{2^j}}\sum_m H_m \int_{T_m}^{\infty} \psi^*\left(\frac{t-k}{2^j}\right)\mathrm{d}t.$$

We will assume that the slowly varying function $s(t)$ coincides with the approximation of the function $f(t)$ with the resolution *J*, and therefore is wholly described by the scaling coefficients $c_J[k]$. Then their contribution to the wavelet coefficients with $j \leq J$ equals zero. These wavelet coefficients, called below clean wavelet coefficients, are completely determined by the locations and heights of the edges, T_m and H_m, and by the template wavelet coefficients $d_j^{\theta}[k]$,

$$d_j^c[k] = \sum_m H_m d_j^{\theta}[k-T_m]. \quad (7)$$

As has been mentioned above, the wavelet and scaling coefficients of the higher octaves (*j* = 1, 2, 3) are corrupted by the noise in a greater extent than those of the lower octaves (*j* = 3, 4, 5). On the one hand, this is explained by the fact that we often have a high-frequency noise. On the other hand, this is due to the signal power concentration in the low frequency component of the signal. Therefore, the signal-to-noise ratio is better in low octaves.

The described peculiarities of wavelet coefficients have led us to a new approach to the filtration of wavelet coefficients. The basic idea of this approach is the following. From the analysis of wavelet coefficients with large octave number *J* one can find positions T_m and heights H_m of the edges for a particular signal. After that, by using the template coefficients $d_j^{\theta}[k]$, one can calculate the clean wavelet coefficients $d_j^c[k]$ with $j \leq J$. These coefficients are used to replace real noisy wavelet coefficients $d_j[k]$ for all *j*. Supplementing the clean wavelet coefficients by the retained scaling coefficients $c_J[k]$ and carrying out the inverse

DWT, we obtain the filtered signal. As a result, the noise is reduced to a large extent, and spurious parasitic oscillations do not arise. Moreover, it should be noted that slow time variations of the signal are modeled correctly, since they are mainly described by the scaling coefficients $c_J[k]$.

The locations of edges, T_m, can be found as the positions of extremes of the wavelet coefficients with sufficiently large octave number $d_J[k]$, and the heights of edges can be calculated from the extreme wavelet coefficients by the expression

$$H_m = \frac{d_J[T_m]}{d_J^{\theta}[0]}. \qquad (8)$$

Some threshold may be used to distinguish the edge peaks from those produced by noise. This threshold defines the minimum height of edges.

It is clear that the octave number J is desired to be taken as large as possible to reduce the noise to a large extent. However, the value of J is restricted by two requirements. Firstly, the approximation with the resolution J should be sufficiently accurate to describe the slowly varying component of the signal. Secondly, with increasing J the resolution of closed edges becomes worse since their edge peaks merge each other. Thus, to distinguish the finest features in the case of weak noise one can take $J = 2, 3$, and in the case of strong noise it should be taken $J = 3, 4$. To improve the resolution of closely situated edges the locations and heights of the edge can be found from the J_1-th octave; the scaling coefficients can be retained at the J_2-th octave, and clean wavelet coefficients can be calculated for $J_2 > J_1$.

Thus, the algorithm of template wavelet coefficients allows the noise reduction not only between the edges, but also in their vicinity, and parasitic oscillations do not arise. Moreover, the algorithm allows reconstructing the sharp edges from smoothed edges corrupted by the noise.

4. Choice of the Wavelet

Let us consider the wavelet in the form of a derivative of an even square integrable function $G(t)$,

$$\psi(t) = \frac{\mathrm{d}G}{\mathrm{d}t}, \qquad G(-t) = G(t).$$

Then the expression (6) for the template wavelet coefficients is reduced to

$$d_j^{\theta}[k] = -\sqrt{2^j}\, G\left(\frac{k}{2^j}\right). \qquad (9)$$

To find the locations and heights of edges with a high accuracy, the edge peaks should be well localized and have a single extreme, pointing the edge location. This means that the function $G(t)$ should have a bell-like shape.

For example, $G(t)$ can be taken in the form of Gaussian. Then the wavelet will be the first derivative of the Gaussian. However, the cubic B-spline is the more appropriate choice for the function $G(t)$,

$$\phi_3(t) = \begin{cases} \frac{1}{6}(t+2)^3, & -2 \le t \le -1, \\ -\frac{1}{6}(3t^3 + 6t^2 - 4), & -1 \le t \le 0, \\ \frac{1}{6}(3t^3 - 6t^2 + 4), & 0 \le t \le 1, \\ -\frac{1}{6}(t-2)^3, & 1 \le t \le 2, \\ 0, & |t| > 2. \end{cases} \qquad (10)$$

The cubic B-spline and the chosen wavelet are shown in Fig. 4. The Fourier transform of the cubic B-spline is

$$\hat{\phi}_3(\omega) = \frac{1}{\sqrt{2\pi}}\left(\frac{\sin\omega/2}{\omega/2}\right)^4.$$

It turns out that for the chosen wavelet exact pyramidal direct and inverse DWT algorithms with the finite-length filters (i. e. the filter with finite number of nonzero elements) can be built. The formulas of the pyramidal DWT can be obtained from the formulas of the undecimated biorthogonal DWT (5) substituting $d_{j+1}[k]$ by $d_j[k]$, $j = 0, 1, 2, \ldots, J-1$, with the filters given in Table 1.

We have obtained this pyramidal algorithm from the well-known biorthogonal MRA with the quadratic B-spline as the scaling function [1] by using the ex-

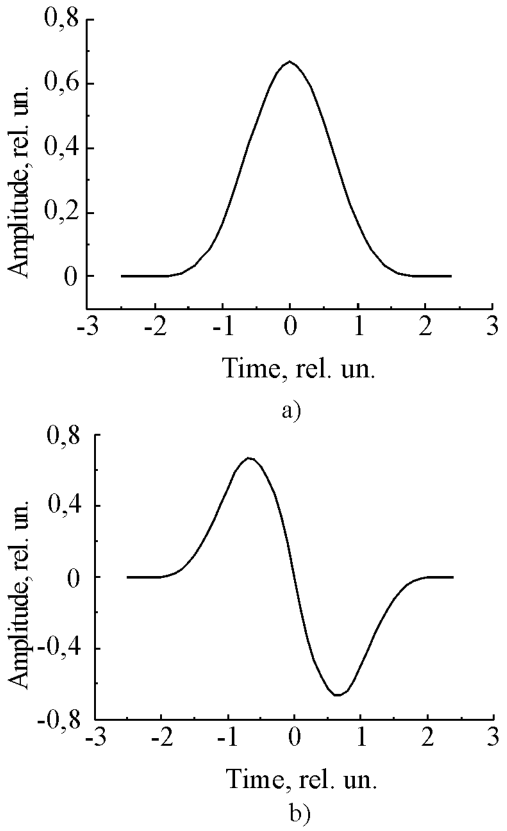

Fig. 4. *Cubic B-spline (a) and proposed wavelet (b)*

pression that relates the chosen wavelet

$$\psi_B = \frac{d\phi_3}{dt}, \qquad (11)$$

to the wavelet ψ_2 from the above mentioned biorthogonal MRA,

$$\hat{\psi}_2(2\omega) = -\frac{1}{2} e^{-i\omega} \left(2 + \cos\omega\right) \hat{\psi}_B(\omega).$$

In other words, the pyramidal algorithm has been obtained substituting the biorthogonal basis of subspaces W_j based on ψ_2 by nonorthogonal basis based on the chosen wavelet ψ_B.

For the chosen wavelet, the template wavelet coefficients can be rewritten as

Table 1. *Filters*

n	$g[n]$	$h[n]$	$\tilde{g}[n]$	$\tilde{h}[n]$	$h_3[n]$
–3	–	–	–1/16	–	–
–2	–	–	–1/16	–	$\sqrt{2}/16$
–1	–	$-\sqrt{2}/4$	1/2	$\sqrt{2}/8$	$\sqrt{2}/4$
0	–1	$3\sqrt{2}/4$	1/2	$3\sqrt{2}/8$	$3\sqrt{2}/8$
1	1	$3\sqrt{2}/4$	1/16	$3\sqrt{2}/8$	$\sqrt{2}/4$
2	–	$-\sqrt{2}/4$	1/16	$\sqrt{2}/8$	$\sqrt{2}/16$

$$d_j^0[k] = -\sqrt{2^j}\,\phi_3\left(\frac{k}{2^j}\right), \qquad (12)$$

and the clean wavelet coefficients (7) are given by

$$d_j^c[k] = -\sqrt{2^j} \sum_m H_m \phi_3\left(\frac{k - T_m}{2^j}\right). \qquad (13)$$

We have found that clean wavelet coefficients can be calculated in a fast way. Namely, since the cubic B-spline is the scaling function of biorthogonal MRA [1], the Eq. (4a) is valid for this spline with the filter $h_3[k]$ (see Table 1). By applying (4a) to the expression (13) one can find that clean wavelet coefficients can be calculated with the Eq. (5a). In fact, it is sufficient to calculate the clean wavelet coefficients $d_0^c[k]$ for $j = 0$ directly from (13), and then take them as the coefficients $c_0[k]$ for (5a). By carrying out the calculation in this way, we have obtained

$$c_j[k] = -\frac{1}{\sqrt{2^j}} \sum_m H_m \phi_3\left(\frac{k - T_m}{2^j}\right) \qquad (14)$$

One can easily see that required clean wavelet coefficients equal

$$d_j^c[k] = 2^j c_j[k], \; j = 1, 2, ..., J-1. \qquad (15)$$

The choice of cubic B-spline as a function $G(t)$ allowed us to build simple, effective and exact direct and inverse pyramidal DWT algorithms with the finite length filters, and to organize the computation of the clean wavelet coefficients in a fast way. Another choice requires more complex algorithms than proposed pyramidal. Therefore, the choice of cubic B-spline can be considered to be particularly successful.

5. Results

Now the final version of the proposed algorithm can be described by collecting all steps discussed in the previous sections. The main steps of the algorithm are shown in Fig. 5. First of all, the wavelet $d_j[k]$ and scaling $c_J[k]$ coefficients are calculated by using the direct DWT with the chosen wavelet (5a, b). Then the edge positions T_m and edge heights H_m are calculated from the coefficients $d_J[k]$, and clean coefficients $d_0^c[k]$ are built according to (13). The other wavelet coefficients are built by using the fast algorithm (14-15). At last, the filtered signal is obtained by using the inverse DWT (5c).

Thus, the application of the proposed noise reduction technique allows us to avoid the excitation of parasitic oscillations. The result of applying the proposed algorithm to a noiseless test signal (see Fig. 2 (a)) is shown in Fig. 2 (c). The result of applying the threshold algorithm to the same noiseless test signal is shown in Fig. 2 (b). As one can see, parasitic oscillations in the vicinity of edges are totally absent when proposed algorithm is used. This is in contrast to the threshold filtering technique.

Moreover, proposed technique allows an effective noise reduction from the signal not only between the edges but in the vicinity of the edges as well. The noisy test signal shown in Fig. 3 (a) was processed by using the threshold technique (Fig. 3 (b)) and the proposed algorithm (Fig. 3 (c)). Comparing both figures one can see that the noise reduction is rather good when the proposed algorithm is used.

The signal processing algorithm described above can be used for grey-level image processing as well. Grey-level images are treated by an application of the one-dimensional algorithm at first to columns and then to strings. The color image can be represented as three images, which are the RGB-components of colors, and thus it can be processed by applying the grey-level image processing algorithm to each of these components.

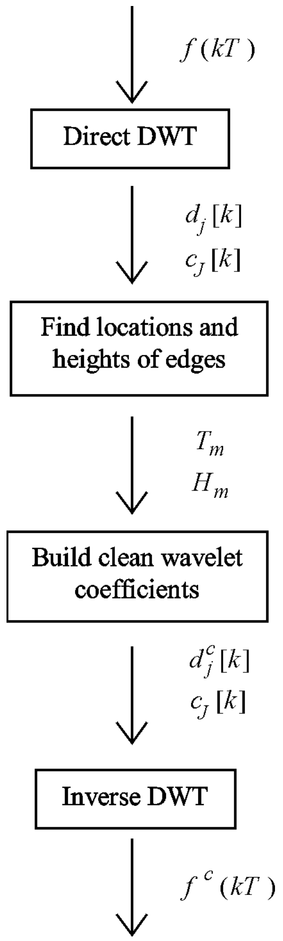

Fig. 5. *The scheme of the noise reduction algorithm based on template wavelet coefficient*

Acknowledgments

The authors thank Prof. D. M. Vavriv for valuable discussions and for careful reading the manuscript. This work was supported in part by EC under Contract ERBIC 15 CT 960816.

References

1. I. Daubechies. Ten Lectures on Wavelet. SIAM, Philadelphia, 1992, 357 pp.
2. Wavelets: Time-Frequency Methods in Phase Space. Proc. of the Int. Conf., Marseille, December 1987. J. M. Combes, A. Grossmann, Ph. Tchamitchian eds., Springer, 1989.
3. M. Holschneider, R. Kronland-Martinet, J. Morlet, Ph. Tchamitchian. Reference [2] above, pp. 286-297.
4. M. J. Shensa. IEEE Trans. Signal Processing. 1992, **40**, pp. 2464-2482.
5. O. Rioul, P. Duhamel. IEEE Trans. Inf. Theory. 1992, **38**, pp. 569-586.

6. S. Mallat. IEEE Trans. Pattern Analysis and Machine Intell. 1989, **11**, pp. 674-693.
7. D. L. Donoho. IEEE Trans. Inf. Theory. 1995, **41**, pp. 613-627.
8. D. L. Donoho, I. M. Johnstone. Preprint. Department of Statistics, Stanford University, 1992. Also Biometrika. 1994, **82**, pp. 425-455.
9. Y. Xu, J. Weaver, D. Healy, J. Lu. IEEE Trans. Image Processing. 1994, **3**, pp. 747-758.

Алгоритм удаления шума на основе использования шаблонных вейвлетных коэффициентов

А. А. Безвесильный, В. В. Виноградов, К. Шунеманн

В статье предложен новый алгоритм, основанный на применении шаблонных вейвлетных коэффициентов для решения проблем, связанных с удалением шума в окрестности границ в сигналах и изображениях и подавлением паразитных осцилляций, которые возникают при использовании пороговых вейвлетных алгоритмов. Показано, что этот подход требует выбора специального вейвлета. Приведены примеры применения предложенного подхода.

Алгоритм видалення шуму на основі застосування шаблонних вейвлетних коефіцієнтів

О. О. Безвесільний, В. В. Виноградов, К. Шунеманн

У статті запропоновано новий алгоритм, що базується на використанні шаблонних вейвлетних коефіцієнтів для розв'язання проблем, пов'язаних з видаленням шуму поблизу меж в сигналах та зображеннях і знищення паразитних осциляцій, що виникають у разі застосування порогових вейвлетних алгоритмів. Зазначено, що цей підхід вимагає вибору спеціального вейвлета. Наведено приклади використання запропонованого підходу.